Cysteine Scanning Mutagenesis at 40 of 76 Positions in Villin Headpiece Maps the F-Actin Binding Site and Structural Features of the Domain†

Don S. Doering‡ and Paul Matsudaira*

Whitehead Institute for Biomedical Research and Department of Biology, Massachusetts Institute of Technology, Nine Cambridge Center, Cambridge, Massachusetts 02142

Received June 28, 1996⊗

ABSTRACT: Villin headpiece, the 76 amino acid, C-terminal domain of villin, is one of the two F-actin binding sites in villin necessary for F-actin bundling activity. Expression and study of recombinant headpiece revealed the domain to be remarkably thermostable (T_m = 74 °C) for a non-disulfide-bonded domain. Forty independent point mutations to cysteine of headpiece have been purified and tested for their actin binding activity, cysteine reactivity, and thermal stability. These assays identify two segments of headpiece, near amino acids 38 and 70 of headpiece, in which mutations to cysteine significantly disrupt cosedimentation of headpiece with F-actin. Assay of the thermal stability of these mutants and assay of the reactivity of the introduced cysteine show that these amino acids are mutations at the protein surface that do not perturb the overall structure of the domain. The actin binding mutants are replacements to cysteine of Lys38, Glu39, Lys65, Lys70, Lys71, Leu75, and Phe76 of headpiece. We propose that these discontinuous segments of charged amino acids define the F-actin binding contacts of the headpiece domain. The assay of mutants for effects on the thermal stability of helical structure as well as the assay of reactivity of the introduced sulfhydryl group identify candidate positions that are involved in the stabilizing core and internal structure of the domain. The cysteine scanning mutagenesis also identifies an amino-terminal subdomain (Val1−Leu35) and a predominantly helical carboxy-terminal subdomain (Pro36−Phe76).

Villin is unique among cytoskeletal proteins because it can both assemble and disassemble filamentous actin structures. In the absence of calcium, villin is a cross-linking protein which organizes actin filaments into bundles which support the microvilli that cover the absorptive surface of intestinal and kidney epithelia, amphibian oocytes, and visceral yolk sac endoderm. However, in the presence of calcium, villin disrupts the organization of the cytoskeleton by severing actin filaments into short fragments. The property of one protein to exhibit both activities is explained by its relationship to two, otherwise distinct, families of actin binding proteins. The calcium-dependent actin-severing activity and the tandem repeats of a conserved 120 amino acid structural domain relates villin to gelsolin, severin, fragmin, adseverin, and scinderin (Andre et al., 1988; Hartmann et al., 1989). The F-actin[1] bundling activity relates villin to the family of bundling proteins that includes fimbrin, dematin, α-actinin, fascin, and others (Matsudaira, 1994; Otto, 1994).

Actin cross-linking activity requires two F-actin binding sites. In villin, one site lies at the junction of the first and second domains (De Arruda et al., 1992). The second site lies in the C-terminal domain, termed headpiece. First discovered as a proteolytically derived F-actin binding fragment of villin, headpiece binds to actin filaments and is necessary for villin's actin cross-linking activity (Glenney & Weber, 1981; Glenney et al., 1981). An oligomeric construct that expresses headpiece fused to the terminus of enzymatically active β-galactosidase suggests that headpiece is also sufficient to be an F-actin bundling site (Doering, 1992). Villin's cross-linking activity stimulates the elongation of microvilli when transfected into cells that normally do not express villin, and this activity appears dependent upon an intact headpiece domain (Friederich et al., 1989; Friederich et al., 1992).

The isolated domain binds to F-actin with a K_d of ~7 μM and binds to F-actin at a saturating ratio of 1:1 with the actin monomer (Glenney & Weber, 1981; Pope et al., 1994). Headpiece does not compete for F-actin binding with villin's first two domains, with gelsolin's second domain, or with α-actinin, suggesting that headpiece binds a different site on F-actin than these proteins (Pope et al., 1994). Headpiece plays no role in severing actin filaments; the six amino-terminal domains retain all of the calcium regulated actin-severing activities of the intact molecule, and headpiece bears no homology to these domains.

The appendage of headpiece at the C-terminus of villin suggests that headpiece originated independently of the actin severing domains and an evolutionary gene fusion event combined the gelsolin-like gene and the headpiece gene. This hypothesis is supported by the discovery of headpiece at the C-terminus of a "protovillin" in dictyostelium and at the C-terminus of an unrelated actin cross-linking protein,

† This work was supported in part by NIH Grant DK35306 to P.M.

* To whom correspondence should be addressed. Phone: (617) 258-5188. Fax: (617) 258-7226. E-mail: matsu@wi.mit.edu.

‡ Current address: AquaPharm Technologies Corp., 9110M Red Branch Road, Columbia, MD 21045. Phone: (410) 720-1018. Fax: (410) 715-1281. E-mail: doering@aquapharm.com.

⊗ Abstract published in *Advance ACS Abstracts,* September 15, 1996.

[1] Abbreviations: bp, base pairs; CD, circular dichroism; DTT, dithiothreitol; DTNB, 5,5′-dithiobis(2-nitrobenzoic acid); EDTA, ethylenediaminetetraacetic acid; F-actin, filamentous actin; GuHCl, guanidine hydrochloride; HPLC, high-performance liquid chromatography; rHP, recombinant chicken villin headpiece; TFA, trifluoroacetic acid; WT, wild-type.

S0006-2960(96)01569-3 CCC: $12.00

```
          1                   20                  40                  60                  76
          •                   •                   •                   •                   •
Hu  VFNANSNLSSGPLPIFPLEQLVNKPVEELPEGVDPSRKEEHLSIEDFTQAFGMTPAAFSALPRWKQQNLKKEKGLF
Mu  VFTANTSLVLGPLPTFPLEELVNKSVEDLPEGVDPSSKEEHLSTEDFTRALGMTPAAFSALPRWKQQNIKKEKGLF
Ch  VFTATTTLVPTKLETFPLDVLVNTAAEDLPRGVDPSRKENHLSDEDFKAVFGMTRSAFANLPLWKQQNLKKEKGLF
Cys -----C-C---C---C-CC--C-CCCCC-CC-CC--CCCCC--CCCCCC---C-CC---C--C-C--C-CCCC-CC
```

FIGURE 1: Sequence comparison of villin headpiece from human (Arpin et al., 1988), mouse (GenBank Accession No. M98454), and chicken (Bazari et al., 1988). Villin headpiece is defined as the peptide produced by cleavage of chicken villin at glutamic acid 749 by V8 protease; the 76 amino acids of the peptide are numbered 1−76 from Val750 of villin. Sequence positions identical in all three species or that are very conserved (Asp-Glu, Ile-Leu, Ser-Thr) are shown in bold type. Nonidentical positions are shown in normal type. Amino acids of chicken villin headpiece uniquely mutated to cysteine in this study are shown (C).

dematin (Hofmann et al., 1993; Rana et al., 1993). The presence of headpiece in three distinct proteins suggests that headpiece has been used to confer a specific F-actin binding activity. Although headpiece is the smallest known F-actin binding domain (76 amino acids), there is little known about its F-actin binding. Deletion and site-directed mutagenesis experiments suggested that a cluster of charges, the KKEK sequence, at the C-terminus is important for actin binding and for stimulation of microvillar growth (Friederich et al., 1992).

We have chosen to probe the structure of headpiece and to map the functional surface of the headpiece domain by the strategy of cysteine scanning mutagenesis. This strategy combines the high resolution of scanning mutagenesis (Cunningham & Wells, 1989; Wells, 1991) with the utility of directed sulfhydryl chemistry (Falke & Koshland, 1987; Falke et al., 1988; Milligan & Koshland, 1988). Cysteine scanning mutagenesis has been extensively applied to transmembrane proteins [for example, Pakula and Simon (1992), Kaback et al. (1994), and Lee et al. (1995)] but not previously to a cytoskeletal protein. There are no cysteines in the sequence of villin headpiece (Figure 1). Thus, every independent replacement of an amino acid by cysteine will introduce a site-specific chemical modification site. The introduced cysteine is also expected to perturb the side-chain interactions in the structural core of the domain and at the actin−headpiece binding interface. Here we report the expression, purification, and partial characterization of chicken villin headpiece and of 40 independent single cysteine mutants of villin headpiece. The structural and functional assays of these mutants identify amino acids that are critical to the structure of the domain and for the F-actin binding function of villin headpiece.

EXPERIMENTAL PROCEDURES

pAED4 Expression Vector. Commercially available plasmids were modified to create a phagemid for protein overexpression, convenient cloning, and mutagenesis. The plasmid backbone of the phagemid/expression vector, pAED4, is pUC-f1 (Pharmacia Fine Chemicals, Piscataway, NJ). Two deletions were made to this backbone: from the *Nde*I to *Kpn*I sites (225 bp) and from the *Sal*I to the second *Pvu*II site (199 bp). The T7 expression sequences of pAED4 are from the pET3a vector (Novagen, Inc., Madison, WI) and were moved into the plasmid after the *Nde*I to *Bgl*II fragment of pSP72 (168 bp) (Promega Inc., Madison, WI) was cloned into the *Nde*I−*Bam*HI site of pET3a. The *Nhe*I to *Bgl*II fragment (551 bp) of the polylinker-modified pET3a was cloned into the *Bam*HI−*Xba*I site of the deleted pUC-f1 to create pAED4; cloning sites were verified by DNA sequencing (Figure 2A).

Construction of the Headpiece Expression Vector. The headpiece gene was isolated and the glutamic acid at the cleavage site was replaced by a methionine at an *Nde*I cloning site in a single step by PCR amplification using mutagenic primers and the chicken villin cDNA as PCR template (Bazari et al., 1988). The 240 bp product was cloned into the pAED4 expression vector/phagemid allowing the overexpression of the 8.5 kDa headpiece domain in *Escherichia coli* BL21(DE3); the sequence of pDDHP10 was verified by DNA sequencing (Figure 2B).

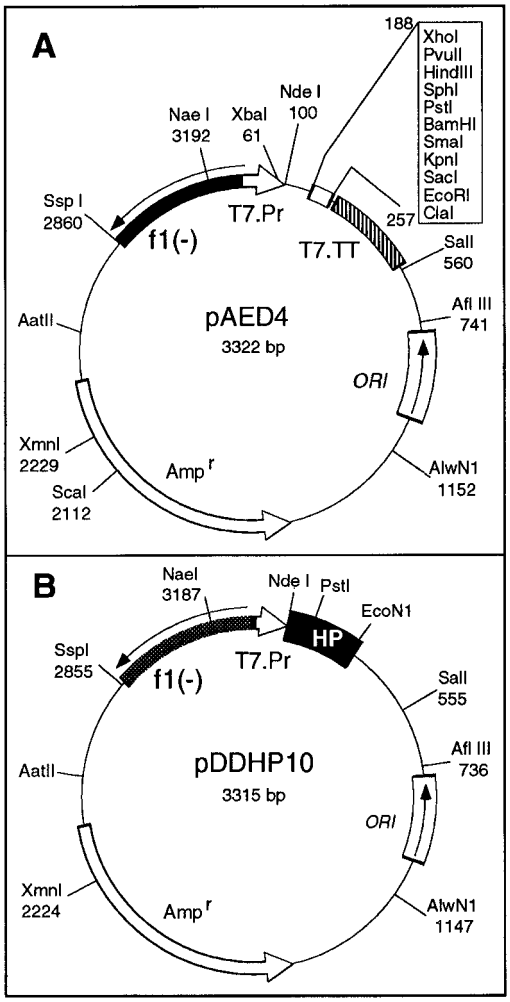

FIGURE 2: Schematic diagrams of (A) the T7 expression vector/phagemid, pAED4, and (B) the villin headpiece vector, pDDHP10. The pUC backbone was modified with a promoter (T7.Pr) and transcriptional terminator (T7.TT) from T7. HP, chicken villin headpiece coding sequence; f1(−), the f1 intergenic region.

Large Scale Purification of rHP. Four liters of *E. coli* BL21(DE3) transformed with the wild-type headpiece expression vector pDDHP10 were induced with 1 mM IPTG. Cells were harvested 5 h postinduction, frozen at −80 °C, lysed by sonication in 50 mM Tris, 0.2 M NaCl, 3 M urea, and 0.1 mM EGTA, pH 8.0, and centrifuged at 70000*g* for 30 min to clarify the lysate. The lysate (100 mL total) was

eluted through a 1.8 L 5 cm × 90 cm AcA34 column (Pharmacia Fine Chemicals, Piscataway, NJ) in the lysis buffer. The headpiece-containing peak was pooled and loaded onto an 80 mL CM-Sepharose column equilibrated in 50 mM Tris, pH 8.0. The flow-through fractions were pooled, dialyzed against water, and concentrated by lyophilization. The dried peptide was suspended in 100 mL of 0.1 M ammonium bicarbonate, pH 8.0, and loaded onto a 25 mL DEAE Sephacyl column equilibrated in the same buffer. Headpiece does not bind to this column and the flow-through fractions were pooled and concentrated by lyophilization. Headpiece was identified by protein sequencing, high-performance liquid chromatography, amino acid analysis, and matrix assisted laser desorption ionization mass spectrometry (MALDI MS) and was identical in structure and molecular weight to headpiece purified by V8 cleavage of purified chicken villin (data not shown).

Cloning into M13 and ssDNA Mutagenesis. The headpiece gene was cloned into M13mp19 and mutagenesis was performed with purified oligonucleotides according to the method of Kunkel (1987). All mutations were verified by sequencing the entire gene with Sequenase (United States Biochemical, Cleveland, OH). Headpiece mutants were then cloned into pAED4 for expression and purification. The cysteine-headpiece mutants are identified by the wild-type amino acid and amino acid number of headpiece, followed by C, e.g., the mutation of valine to cysteine at headpiece position 25 is designated either Val25C or V25C.

Small Scale Purification of Mutants. Cells from 250 mL cultures of headpiece cysteine mutants were frozen and then lysed by sonication in 10 mM Tris-HCl, pH 8.5, 50 mM NaCl, 0.1 mM EDTA, and 1 mM DTT. The lysate was clarified by centrifugation at 10 krpm for 5 min (15000*g*) and then at 100 krpm for 10 min at 4 °C in a Beckman TL-100 ultracentrifuge, and the supernate was loaded onto a 0.8 × 40 cm G-75 column in the lysis buffer. The peak fractions were pooled, dialyzed against water, and lyophilized. The lyophilized G-75 pool was suspended in 0.1 M ammonium bicarbonate, pH 8.0, and eluted through a 1 mL DEAE-Sephacyl (Pharmacia Fine Chemicals, Piscataway, NJ) and lyophilized. The lyophilized DEAE flow-through was suspended in water and centrifuged at 20000*g*, and the supernatant was stored at −20 °C in 5 mM HCl (pH 2.0). Headpiece cysteine mutants were >95% purity as assayed by analytic HPLC (data not shown).

HPLC Analysis. Dried peptides were suspended in 0.1% trifluoroacetic acid (TFA) in water and analyzed on a 2.1 × 250 mm Vydac C18 column on a Hewlett Packard 1090M HPLC instrument (Hewlett Packard, Paramus, NJ). Samples were eluted at 0.2 mL/min with a 0.3% CH_3CN/min gradient of 0.1% TFA to 0.085% TFA/80% CH_3CN. Absorbance was monitored at 230 nm.

Amino Acid Analysis and Mass Spectrometry. Mass spectral data for the comparison of recombinant headpiece and "proteolytic" villin headpiece were obtained by matrix-assisted laser desorption ionization (MALDI MS) time-of-flight mass spectrometry and were kindly provided by the MIT Mass Spectrometry facility. Amino acid analysis was performed at the MIT Department of Biology Biopolymers Laboratory.

Ellman's Assay for Cysteine Reactivity. Headpiece mutants were reduced in 25 mM NaCl, 1 mM EDTA, 40 mM DTT, and 0.1 M phosphate (pH 7.4) and desalted over a 10 mL G-10 column equilibrated in 25 mM NaCl, 1 mM EDTA, and 0.1 M phosphate, pH 7.4, to remove DTT. Conditions were established so that the concentration of peptide in the peak fraction was approximately 25 μM. This fraction was collected and immediately placed in a stirred cell in an Aviv model 14DS UV−vis−IR spectrophotometer (Lakewood, NJ). 5,5′-Dithiobis(2-nitrobenzoic acid) (3 mM) (DTNB) (Pierce Chem. Co., Rockford, IL) was added to a final concentration of 60 μM. The change in absorbance at 412 nm was measured at 1 s intervals until the sample had reached equilibrium. After background subtraction, the time after addition of DTNB at which the sample reached half maximal absorbance was calculated ($T_{1/2}$).

Circular Dichroism Thermal Denaturation. Approximately 350 μg of peptide was dissolved and reduced in 25 mM NaCl, 2 M guanidine hydrochloride, 50 mM DTT, 0.1 mM EDTA, and 10 mM sodium phosphate, pH 7.4. DTT was removed on a 10 mL G-10 column equilibrated in 25 mM NaCl, 2 M guanidine hydrochloride, 0.5 mM DTT, 0.1 mM EDTA, and 10 mM sodium phosphate, pH 7.4. The peptide was collected as a 2.5 mL fraction of approximately 20 μM headpiece and immediately assayed. Melts were monitored at 222 nm from 5−80 °C in 3 °C steps with an Aviv 62DS circular dichroism spectrometer. At each temperature, the sample was equilibrated for 2 min, and the signal was recorded with a 15 s averaging time. The transition midpoint values (T_m) were determined by examination of the derivative of $\{\theta\}_{222}$ with respect to the reciprocal of the temperature (Cantor & Schimmel, 1980).

F-Actin Pelleting Assay. Equal weights of each headpiece mutant and wild-type headpiece were dried and suspended in a small volume with a 100-fold molar excess of DTT, allowed to reduce, and then diluted to 100 μL by the addition of F-actin and buffer to final concentrations of 45 μM cysteine-headpiece, 26 μM actin, 100 mM NaCl, 1 mM $MgCl_2$, 0.1 mM ATP, 5 mM DTT, and 10 mM Tris, pH 7.4. Duplicate samples were incubated at room temperature for 4−6 h and then centrifuged at 300000*g* for 1 h at 4 °C in a Beckman TL-100 microultracentrifuge. After centrifugation, supernates (G-actin and unbound peptide) and pellets (F-actin and the bound peptide fraction) were separated and brought to equal volumes in SDS−PAGE sample buffer.

Densitometry and Pelleting Assay Analysis. The sedimented and supernatant fractions of each duplicated sample were analyzed by SDS−PAGE with an internal headpiece concentration series to calibrate each gel. After destaining, the amount of protein in each band was calculated by densitometry of the gels using a Molecular Dynamics 300 Series volume densitometer (Molecular Dynamics, Sunnyvale, CA). The mean fraction of headpiece mutants sedimented under identical conditions were compared to the mean of eight measurements of the wild-type headpiece and the standard deviation of the measurement of the wild-type domain.

RESULTS

Purification of Recombinant Headpiece. In *E. coli* BL21-(DE3) transformed with the wild-type headpiece expression vector, pDDHP10, IPTG induced the overexpression of an 8.5 kDa protein, as judged by SDS−PAGE (Figure 3, inset) (Studier & Moffat, 1986; Rosenberg et al., 1987). Maximal expression was achieved 5 h postinduction, and the product

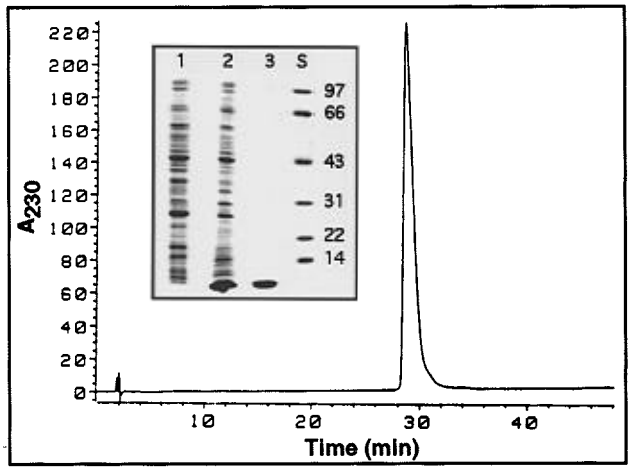

FIGURE 3: Analytic reverse-phase HPLC of recombinant headpiece (rHP) monitored at 230 nm. Inset shows SDS−PAGE of (1), the total bacterial lysate without induction of headpiece expression, (2) total bacterial lysate after induction, and (3) final purified rHP; s, molecular weight standards (kDa).

was stable in culture for at least 8 h. On immunoblots of the bacterial lysate (data not shown), the 8.5 kDa protein cross reacted with a polyclonal antisera, R200.2, that is specific for the chicken villin headpiece (Matsudaira et al., 1985).

After sequential size exclusion and ion exchange chromatography, the purified 8.5 kDa protein was analyzed by mass spectrometry and reverse-phase HPLC (Figure 3) and judged to be pure. By MALDI MS, the mass of recombinant headpiece was determined to be 8535.0 ± 1.3 mass units in six determinations as compared to 8534.7 ± 1.6 mass units for headpiece purified from chicken villin; the weight predicted by the amino acid sequence is 8535. On reverse-phase HPLC, recombinant headpiece eluted as a single peak with purity >99% (Figure 3). A single 4 L prep yielded nearly 300 mg of headpiece. This single preparation has been used for all of the structural and functional characterization of wild-type headpiece described in this study. The purity of the mutants after size exclusion chromatography and a single ion exchange column was comparable with the wild-type headpiece. By HPLC, mutant headpiece was >95% pure but in some preparations, two closely eluting peaks were detected by reverse-phase HPLC. Analysis by MALDI MS and protein sequencing indicated the later eluting peak contained the mutant peptide that included an N-terminal methionine. This peak comprised <10% of the total protein. The high expression levels (75 mg/L) of the domain and its mutants appears reflective of its high solubility and stability.

Headpiece Is a Highly Stable Domain with an α-Helical Subdomain. The conformation of headpiece was studied by circular dichroism (CD) spectroscopy to characterize wild-type headpiece and to establish a structural assay for the comparison of the mutants with wild-type headpiece. At 25 °C, the CD spectrum of recombinant headpiece (Figure 4A) showed two minima at 208 and 222 nm. These minima indicate that headpiece contains α-helical secondary structure, and its α-helical content is predicted to be approximately 30%. The conformational stability of the folded domain was measured by monitoring the CD signal at 222 nm as the temperature increased from 5 to 80 °C (Figure 4B). Although the domain did retain some α-helical secondary

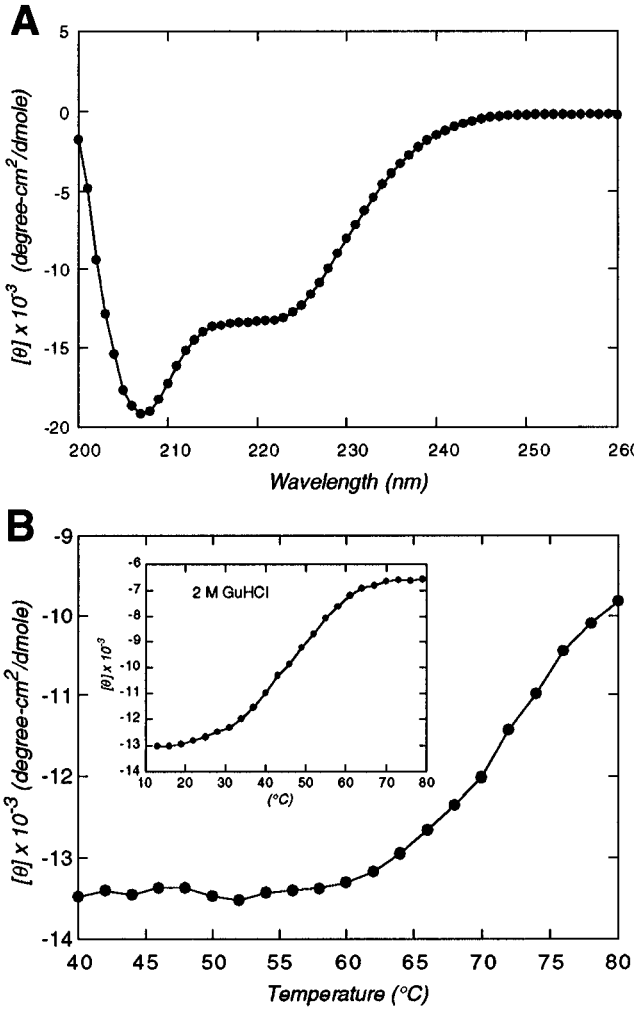

FIGURE 4: Circular dichroism spectrum and thermal unfolding of wild-type headpiece. (A) The CD spectrum of headpiece shows two minima at 208 and 222 nm. (B) The ellipticity at 222 nm does not vary between 5 and 60 °C. Above 60 °C, the ellipticity increases but does not reach a constant value by 90 °C. (B, inset) In 2 M GuHCl, the ellipticity increases at a lower temperature, reaches a stable maximum by 70 °C, and exhibits a T_m of 45.5 °C.

structure above 80 °C, a T_m of 75 °C was estimated from the derivative of the curve. To observe the full transition to an unfolded conformation, thermal denaturation was performed in 2 M guanidine hydrochloride (GuHCl). Under this condition (Figure 4B; inset), the T_m was 45.5 °C, and at high temperatures headpiece showed a random coil conformation. The domain unfolded with a smooth single transition; lowering the temperature from 80 to 5 °C caused the domain to renature completely and the denaturation and renaturation curves had identical T_m's.

Creation and Purification of Headpiece Cysteine Mutants. Of the 76 amino acids in headpiece, a single cysteine was placed at 40 positions to create 40 cysteine mutants. The cysteine scan included 18 of the 19 charged amino acids, and the largest "gap" without a mutation was three amino acids. Highly expressing clones were identified for all of the mutants, and all 40 mutants were isolated from the soluble fraction of a bacterial lysate in a simple two-step purification. None of the 40 mutants formed inclusion bodies or displayed abnormal protease susceptibility. Five mutants, Phe2C, Pro10C, Glu14C, Pro17C, and Phe51C, were expressed at high levels but were not used in this study due to heterogeneity as detected by HPLC. These five mutants are likely

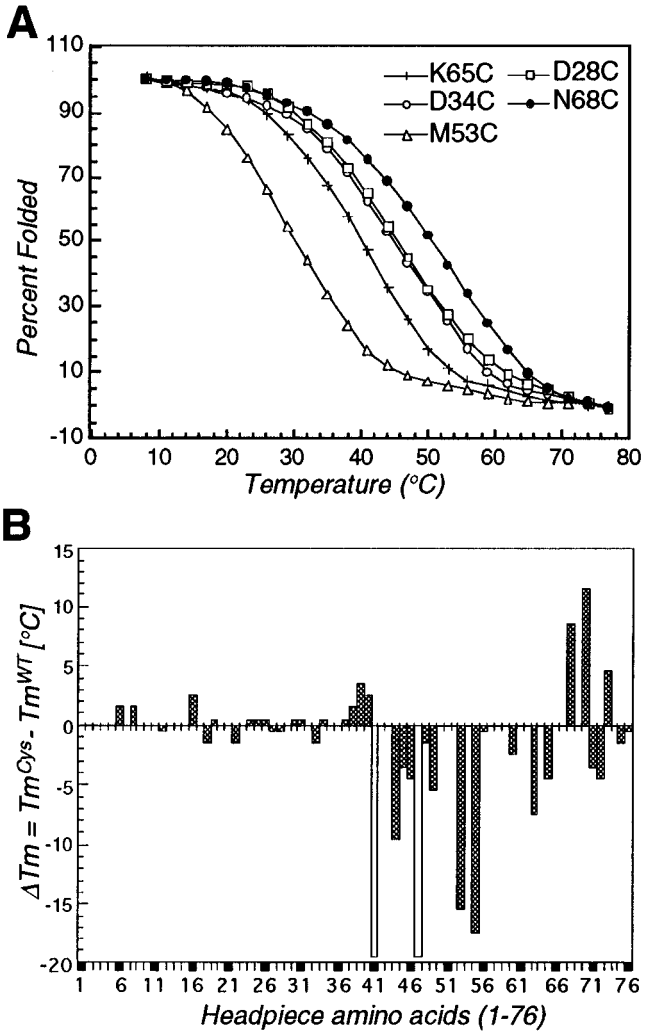

FIGURE 5: Thermal unfolding of headpiece cysteine mutants monitored by circular dichroism. (A) Normalized circular dichroism signal at 222 nm during thermal denaturation of five mutants showing representative mutants of the classes of stability; very unstable (M53C), mildly unstable (K65C), wild type (D28C, D34C), and stabilized (N68C). (B) Summary plot of the change in T_m (°C) of the 40 cysteine mutants expressed as the difference between the mutant and wild-type thermal denaturation transition midpoint temperature.

to be protease sensitive mutants due to disruption of hydrophobic structures (Phe2C and Phe51C) or of turns in the tertiary structure of the peptide chain (Pro10C, Glu14C, and Pro17C).

Characterization of Mutant Stability by Circular Dichroism. At 25 °C, the CD spectra of all the mutants in aqueous solution were identical to the CD spectrum of the wild-type headpiece domain. To characterize the folded conformation of the mutants more carefully, we compared the thermal stabilities of all the mutants. Because the wild-type T_m of headpiece is high, we measured the T_m for each mutant in the presence of 2 M GuHCl, which lowers the T_m of wild-type (T_m^{wt}) headpiece to 45.5 °C. The stability of the mutants were grouped into four classes: wild-type, mildly unstable, very unstable, and stabilized (Figure 5A). Mutants considered to be significantly stabilized are those with a T_m^{cys} that is greater than T_m^{wt} by 6 °C, and significantly destabilized mutants had a measured T_m^{cys} that is less than T_m^{wt} of 6 °C. All mutants showed wild-type CD intensity when returned to 5 °C, indicating that they were fully folded.

Twenty-one of the twenty-five mutants in the wild-type class (T_m's from 43 to 49 °C) were located in the N-terminal half of headpiece. No mutation in this region resulted in a change in the apparent T_m of the mutant headpiece. In contrast to the N-terminus, a mixture of thermal stabilities was detected in the C-terminal half of headpiece (Figure 5B). Four mutants had wild-type T_m. Six mutants were mildly destabilized by the mutation to cysteine (T_m^{cys} is less than T_m^{wt} of 3.5−5.5 °C), E45C, D46C, A49C, K65C, K71C, and E72C, while two other mutants, D44C and L63C, were less stable than wild-type by 9.5 and 7.5 °C, respectively. Two mutants, M53C and R55C, were greatly destabilized (T_m is less than 28−30 °C). The mutants H41C and F47C were almost completely unfolded in 2 M GuHCl. In aqueous solution, their T_m's were 51 and 54 °C, respectively. The unfolding transition did not appear to have begun in aqueous solution at 25 °C, the temperature of the Ellman's assay and actin-binding assays.

Only three mutants clearly showed that the mutation to cysteine increased the stability of the domain. K73C increased the T_m by 4.5 °C to 50 °C, N68C increased the T_m by 8.5 °C to 54 °C, and the most stable mutant, K70C had a T_m 11.5 °C greater than wild-type, of 57 °C. All three mutants lie near the C-terminus of the domain.

Cysteine Reactivity. The chemical reactivity to Ellman's reagent, 5,5′-dithiobis(2-nitrobenzoic acid) (DTNB), was determined for each cysteine mutant to determine the solvent accessibility of cysteine at different positions in headpiece. The time after the addition of DTNB at which the sample reached half-maximal absorbance, $T_{1/2}$, was used to characterize the reactivity of each cysteine mutant (Table 1). The typical time course of the three reactive classes are shown in Figure 6A. Eighteen mutants had "rapid" reactivities ($T_{1/2}$ = 1−3 s), fourteen mutants had "intermediate" reactivities ($T_{1/2}$ = 5−15 s), and eight mutants had "slow" reactivities ($T_{1/2}$ = 25−1000 s) (Figure 6B).

The 18 most reactive mutants define the set of positions at which the introduced cysteine side chain is accessible to DTNB modification. Twelve of these mutants are replacements for polar or charged amino acids and are expected to be exposed to solvent (D19C, D34C, K38C, E39C, D44C, E45C, D46C, S56C, K65C, N68C, K70C, and E72C) while six are substitutions for hydrophobic positions (L8C, F16C, L18C, P30C, L63C, and L75C). Six mutants (L63C, K65C, N68C, K70C, E72C, and L75C) in the highly reactive class lie at the extreme carboxy terminus of the peptide. The intermediate reactive class of mutants were distributed throughout the headpiece sequence and represent a mixture of substitutions for hydrophobic, polar, and charged positions (T6C, K12C, A26C, E27C, D28C, V33C, N40C, H41C, K48C, A49C, R55C, N60C, K71C, and F76C).

The slow reactive mutants were easily distinguishable from the other two classes of mutants by their extremely slow DTNB reaction rates. The reaction of these mutants over time probably corresponds to the slow trapping of cysteine by DTNB as the peptides unfold. V22C, T24C, and A25C were all relatively inaccessible to DTNB and lie within a hydrophobic region from V20 to A26. Two arginine to cysteine substitutions, R31C and R37C, were also slowly reactive and are both flanked by rapidly reactive positions at P30 and K38. M53C is protected from modification and is the last position is a purely hydrophobic region from A49

Table 1: Summary Reactivity, Thermal Stability, and Relative F-Actin Binding Activity of the Headpiece Cysteine Mutants[a]

mutant	$T_{1/2}$	T_m	% WT AB	mutant	$T_{1/2}$	T_m	% WT AB	mutant	$T_{1/2}$	T_m	% WT AB
wild type		46	1.0	R31C	27	46	0.99	M53C	95	30	0.87
T6C	4	47	0.94	V33C	14	44	0.93	R55C	8	28	0.83
L8C	3	47	0.97	D34C	1	46	1.0	S56C	2	45	0.92
K12C	6	45	0.88	R37C	135	46	0.89	N60C	10	43	0.82
F16C	3	48	0.74	K38C	2	47	0.30	L63C	2	38	0.76
L18C	2	44	0.93	E39C	1	49	0.64	K65C	1	41	0.43
D19C	2	46	0.98	N40C	6	48	0.99	N68C	2	54	0.85
V22C	160	44	1.0	H41C	7	51[b]	0.87	K70C	3	57	0.23
T24C	165	46	0.94	D44C	1	36	1.0	K71C	6	42	0.39
A25C	29	46	0.88	E45C	1	42	1.0	E72C	1	41	0.90
A26C	7	46	0.92	D46C	2	41	1.0	K73C	700	50	0.83
E27C	9	45	0.97	F47C	31	54[b]	0.68	L75C	3	44	0.52
D28C	11	45	0.92	K48C	5	44	0.88	F76C	9	45	0.18
P30C	3	46	0.89	A49C	7	40	0.97				

[a] $T_{1/2}$, half maximal cysteine DTNB modification time (seconds); T_m, circular dichroism thermal unfolding midpoint temperature (°C) in 2 M guanidine hydrochloride; % WT AB, relative percentage of wild-type headpiece peptide co-sedimented with F-actin. [b] H41C and F47C were unfolded in 2 M GuHCl. The value shown is without guanidine and compares to the wild-type value of 74 °C.

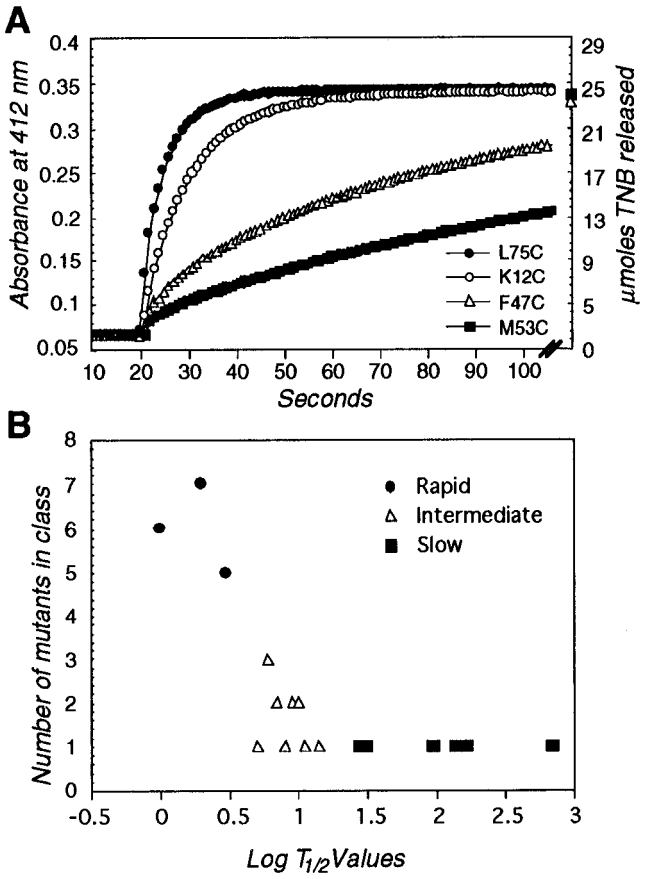

FIGURE 6: Representative data for the chemical reactivity of headpiece cysteine mutants (A) The time course of reaction of four headpiece cysteine mutants with DTNB; L75C (fast), K12C (intermediate), and F47C and M53C (slow). Values on far right of axis show F47C and M53C at equilibrium (B) The classification of headpiece cysteine mutants by reactivity to DTNB. The number of mutants for each log $T_{1/2}$ is plotted: fast reactivity (solid circles), intermediate reactivity (open triangles), and slow reactivity (solid squares).

to T54. One mutant at the carboxy terminus, K73C, was the least reactive mutant and is the last charged position of headpiece.

F-Actin Cosedimentation Assays of the Cysteine Mutants. The actin binding activity of the mutants was compared by their ability to cosediment with F-actin at a fixed condition of headpiece and actin concentration. Under the established conditions, 44% ± 4% ($n = 8$) of wild-type headpiece was found cosedimented with F-actin. Only those mutants whose mean actin-bound fraction was two standard deviations below the mean value of the wild-type (corresponding to <80% of wild-type activity) were considered actin-binding mutants (Figure 7). Mutants that have significantly reduced actin binding activity are K38C, E39C, F47C, K65C, K70C, K71C, L75C, and F76C. The mutants with the next most reduced actin binding activity are F16C, and L63C. An additional 11 mutants are within 1−2 standard deviations of the wild-type value, but this is within the deviation of these measurements and the affinity of these mutants for actin cannot be judged in this single-point assay. Every one of the positions that greatly reduced actin binding when mutated to cysteine is identical among chicken, mouse, and human villin headpiece (Figure 1).

DISCUSSION

Cysteine Scanning Mutagenesis. The highly stable folded conformation of headpiece and the small cysteine side chain allows us to place cysteines at selected positions in the domain without large global affects on structure. We can also exploit the introduced sulfhydryl group to map the surface residues of the domain. In combination with circular dichroism and functional assays, we have identified sets of specific residues that are likely to be responsible for critical structural and functional interactions (Figure 8). Defining the surface of headpiece by the reactivity of the introduced cysteine may be subject to overestimation or underestimation of the solvent-exposed surface. Some of the cysteine substitutions may result in local chain perturbations that might partition the sulfhydryl group onto the surface or into the core in a nonnative conformation without any effect on global stability or structure. The set of headpiece−cysteine mutants provides a valuable set of tools for future studies that utilize the reactive cysteine including mapping cross-links, studying folding transitions, X-ray crystallography, and structural probes such as spin labels and fluorescent probes.

Most interfaces between globular proteins occur at a single surface patch that is almost always composed of discontinuous protein sequences (Fanning et al., 1986; Wells, 1991; Barlow et al., 1986). The protein−protein interface is made of side chains of all types and involves hydrophobic and hydrophilic side chains and all types of molecular interactions. Though protein binding sites are packed as tightly as

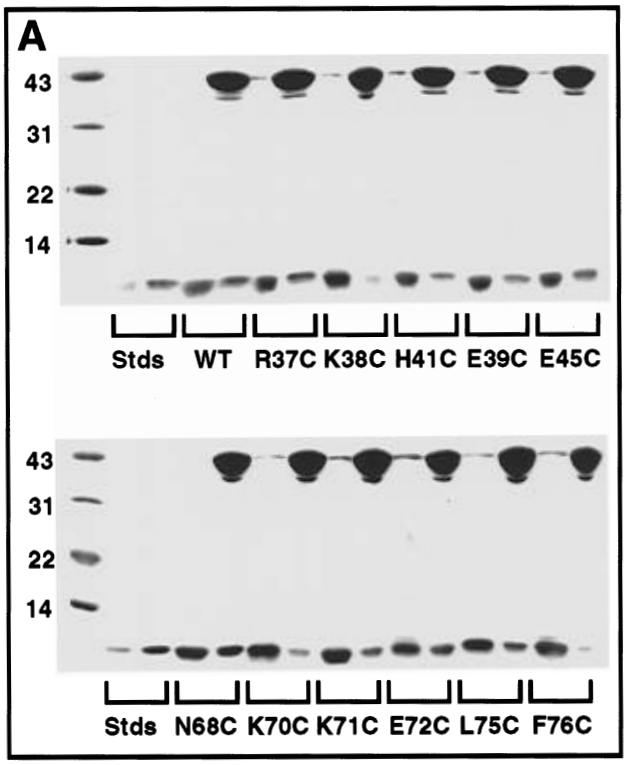

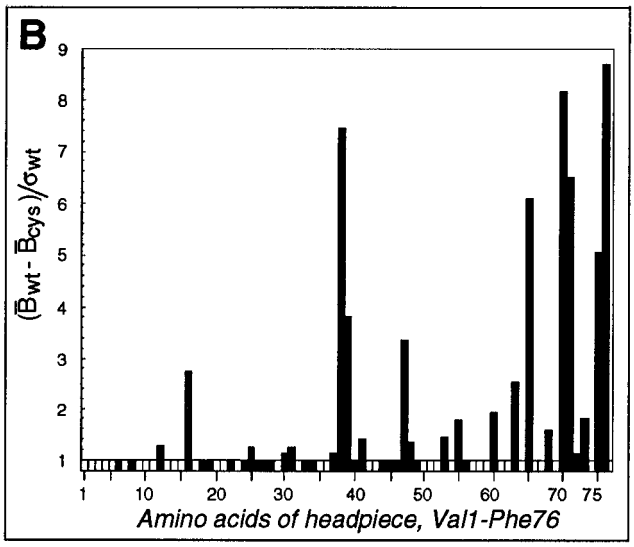

FIGURE 7: F-actin cosedimentation binding activity of headpiece cysteine mutants. (A) Representative SDS−PAGE of samples from the cosedimentation assay of wild-type (WT) and cysteine mutants. Each pair of lanes represent a sample of the supernatant fraction (left) and the sedimented fraction (right) for the indicated mutants. (B) Differences in mean actin-bound fraction between mutant (B_{cys}) and wild-type headpiece (B_{wt}) are expressed in standard deviations (σ_{wt}) of the wild-type measurement. The black boxes on the horizontal axis indicate mutants that were assayed and found to be within one standard deviation of wild type.

the protein interior, the structural core of a protein generally involves more short and long-range stabilizing interactions. A mutation to cysteine in most regions of a protein may be compensated for by minor perturbations and adjustments to the overall structure. However, a change to a cysteine side chain at the protein−protein interface is likely to have a measurable effect on the specificity and affinity of the interaction, and binding function is a more stringent criterion for structure than global stability.

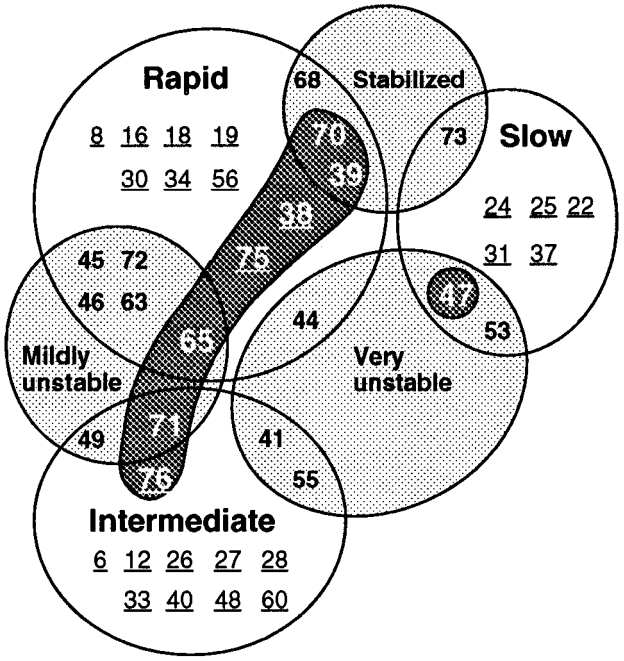

FIGURE 8: Venn diagram of the results of the cysteine scanning mutagenesis. The cysteine mutants are represented by their position number in the wild-type headpiece sequence. Mutants are illustrated in overlapping sets: three classes of Ellman's reactivity (rapid, intermediate, and slow), four classes of stability (wild-type, stabilized, mildly unstable, and very unstable), and mutants with wild-type stability are underlined. Finally, the eighth set is the actin binding mutants, indicated in white numbers.

N- and C-Terminal Subdomains of Villin Headpiece. Our analysis of headpiece structure reinforces the evidence from proteolysis of villin that headpiece is an independently folded domain and provides new information of the domain's substructure and topology. Our studies reveal that headpiece has a remarkably high thermal stability for a non-disulfide-bonded domain and a melting temperature higher than other well-characterized a-helical motifs such as the GCN4 leucine zipper (O'Shea et al., 1989). The small size of the domain, 76 residues, and the high stability against thermal denaturation suggest that headpiece is folded into a unusually compact and stable conformation.

An unexpected finding of our study is the apparent division of headpiece into amino- and carboxy-terminal subdomains. Based on cysteine mutations throughout the headpiece sequence, mutations in the C-terminal half of headpiece affect both stability of the domain and its actin-binding activity while mutations in the N-terminal half have no affects on either of these properties. The apparent wild-type stability of cysteine mutations in the amino-terminus (residues 1−35) of headpiece is surprising. It is possible that mutations in this region may destabilize or stabilize the subdomain, but these changes (1) do not effect the overall stability of the domain and (2) are not detectable by circular dichroism. This region clearly has a tertiary structure, as evidenced by its protease resistance and the partial or complete protection of several cysteine residues in the mutants from chemical modification (e.g., Val22C, Thr24C, and Ala25C). Our interpretation of these observations is that the N-terminal half of headpiece may not be helical and that mutations in this region do not influence the folding and global stability of the carboxy half of headpiece. In contrast to mutations in the N-terminal half, all of the cysteine mutants that stabilize or destabilize headpiece as measured by circular

dichroism thermal denaturation curves are within residues 36−76. This difference in thermal stability between the N- and C-terminal halves hints at the existence of structural subdomains in villin headpiece. The prediction of subdomains from cysteine scanning mutagenesis has subsequently been confirmed by the discovery of a trypsin resistant subdomain, HP-45, from Gly32 to Phe76 of headpiece and the finding that virtually all of the helical content of headpiece can be attributed to helices revealed by NMR in the region from Leu42 to Phe76 (McKnight et al., 1996). A smaller peptide from Pro55 to Phe76 (P22) of human villin is unstructured in aqueous solution but forms an α-helix in the last 10 amino acids in trifluoroethanol (Simenel et al., 1995).

Mapping of the Actin Binding Site Residues. The F-actin cosedimentation assays of the cysteine−headpiece mutants have identified 10 mutants that significantly reduce actin binding: Phe16C, Lys38C, Glu39C, Phe47C, Leu63C, Lys65C, Lys70C, Lys71C, Leu75C, and Phe76C. These positions are distributed throughout the headpiece sequence, and mutations at these sites exhibit different chemical reactivities and effects on folded conformation. Amino acids at an actin binding site must lie on the surface of the domain and be freely accessible to solvent. This requirement predicts that cysteine mutations at these positions will be (1) highly reactive, (2) have minimal effect on conformation, and (3) inhibit actin binding activity. Of the eight mutants which are very reduced in F-actin binding activity, our mutagenesis screen identifies five positions, Lys38, Glu39, Lys65, Lys70, and Leu75, which conform to these three criteria. Two other mutants, Lys71 and Phe76, are slightly less reactive but are likely to be at the actin binding site. Leu63 has reduced actin binding activity, but this mildly unstable mutant may reflect that this leucine, situated between Pro62 and Trp64, is involved in hydrophobic interactions that stabilize the carboxy-terminal helices and reduces actin binding by slight perturbation of the adjacent binding site. It is interesting that our study suggests that Leu75 and Phe76 play a role in the binding site, since phosphorylation of a serine at the equivalent position to villin headpiece Gly74 in dematin headpiece modulates actin binding activity (Azim et al., 1995).

Phe16 reduces actin binding activity near the reliable limits of the single-point sedimentation assay. This phenylalanine may play a role in internal hydrophobic interactions that are not detectable by circular dichroism and which effect the actin binding contacts or, though distant in primary structure, Phe16 is at or near the actin binding site(s) in the tertiary structure. Phe47 is not likely to be a binding site position since a cysteine at this position was relatively inaccessible to DTNB and severely destabilized the domain. It is certainly possible that amino acids that are structurally important and those that are functionally critical are not mutually exclusive.

The actin binding mutants define two regions, the middle of the headpiece sequence and the C-terminus of headpiece, which contribute binding site interactions. We hypothesize that these sequence positions comprise either a single F-actin binding site formed by these two discontinuous peptide segments or comprise two sites by which headpiece binds to F-actin. The clustering of the actin binding mutants at the hydrophilic region of Lys38 and Glu39, and in the carboxy terminus, but the presence of closely juxtaposed mutants with wild-type actin binding activity suggest that these functional mutants are not merely structural aberrations. The large number of mutants that have been analyzed argue against there being another region of headpiece that makes a significant number of contacts with the F-actin filament.

Role of the KKEK Sequence. Our observations augment previous work that implicated only the C-terminal KKEK sequence in human villin (positions 70−73) in actin binding. The carboxy-terminal KKEK (residues 70−73) was proposed to be the actin binding site based upon C-terminal truncations of the domain and studies of synthetic peptides (Friederich et al., 1992). The effects of peptides and charge-reversed mutant peptides in 20-fold molar excess of actin upon cosedimentation and polymerization implicated the KKEK sequence in actin binding. This identification includes the subset of positions identified in our study but also includes two positions which our mutagenesis experiments have excluded (E72 and K73) and excludes Leu75 and Phe76. A structural role for Lys73C is suggested by the lack of reactivity of the cysteine and the stabilization of the domain.

Our observations suggest that the results of peptide binding studies and deletion mutagenesis experiments have not completely identified headpiece−actin binding residues. In deletion mutagenesis experiments, the conformational effects of the mutations were not examined, and our results suggest that truncation of Lys70 to Phe76 or Gly74 to Phe76 would destabilize the headpiece domain. Second, at a 20−40-fold molar excess of peptide, the resulting K_d of 100 μM for P22 (human headpiece Pro55 to Phe76) may be due to trapping of the peptide by F-actin sedimentation and nonspecific interactions. In peptide binding studies, the effects of single amino acid substitutions become enhanced in the absence of three-dimensional structure and the structural influence of other positions remote from the binding sequence. Similar peptides of chicken villin are not reported to show actin binding (J. McKnight, personal communication). Our result that discontinuous peptide segments K38-E39-K70-K71 (K-E, K-K) make critical binding contacts with actin in intact, folded headpiece may explain why peptide mimetic experiments of similarly charged, but probably unstructured peptides exhibit binding constants one order of magnitude lower than that of headpiece. Our studies point to the importance and power of correlative structural and functional analysis in the mapping of discontinuous binding site residues.

ACKNOWLEDGMENT

We thank Drs. B. Tidor, P. Kim, J. McKnight, K. Collins, M. de Arruda, T. Nakayama, R. Ezzell, and J. Lopez for valuable discussions. This study was submitted as partial fulfillment for the requirements of a Ph.D. to the faculty of the Department of Biology, MIT.

REFERENCES

Andre, E., Lottspeich, F., Schleicher, M., & Noegel, A. (1988) *J. Biol. Chem. 263*, 722−727.

Arpin, M., Pringault, E. Finidori, J., Garcia, A., Jeltsch, J. M., Vandekerckhove, J., & Louvard, D. (1988) *J. Cell Biol. 107*, 1759−1766.

Azim, A., Knoll, J., Beggs, A., & Chishti, A. (1995) *J. Biol. Chem. 270*, 17407−17413.

Barlow, D. J., Edwards, M. S., & Thornton, J. M. (1986) *Nature 322*, 747.

Bazari, W. L., Matsudaira, P., Wallek, M., Smeal, T., Jakes, R., & Ahmed, Y. (1988) *Proc. Natl. Acad. Sci. U.S.A. 85*, 4986−4990.
Cantor, C. R., & Schimmel, P. R. (1980) in *Biophysical Chemistry*, Freeman and Co., New York.
Cunningham, B. C., & Wells, J. A. (1989) *Science 244*, 1081−1085.
De Arruda, M. V., Bazari, H., Wallek, M., & Matsudaira, P. (1992) *J. Biol. Chem. 267*, 13079−13085.
Doering, D. S. (1992) Ph.D. Thesis, Massachusetts Institute of Technology, Cambridge, MA.
Falke, J. J., & Koshland, D. E., Jr. (1987) *Science 237*, 1596−1600.
Falke, J. J., Dernburg, A. F., Sternberg, D. A., Zalkin, N., Milligan, D. L., & Koshland, D. E., Jr. (1988) *J. Biol Chem. 263*, 14850−14858.
Fanning, D. W., Smith, J. A., & Rose, G. D. (1986) *Biopolymers 25*, 863.
Friederich, E., Vancompernolle, K., Huet, C., Goethals, M., Finidori, J., Vandekerchove, J., & Louvard, D. (1992) *Cell 70*, 81−92.
Friederich, E., Huet, C., Arpin, M., & Louvard, D. (1989) *Cell 59*, 461−475.
Glenney, J. R., & Weber, K. (1981) *Proc. Natl. Acad. Sci. U.S.A. 78*, 2810−2814.
Glenney, J. R., Geisler, N., Kaulfus, P., & Weber, K. (1981) *J. Biol. Chem. 256*, 8156−8161.
Hartmann, H., Noegel, A. A., Eckerskorn, C., Rapp, S., & Schleicher, M. (1989) *J. Biol. Chem. 264*, 12639−12647.
Hofmann, A., Noegel, A., Bomblies, L., Lottspeich, F., & Schleicher, M. (1993) *FEBS Lett. 328*, 71−76.
Kaback, H. R., Frillingos, S., Jung, H., Jung, K., Prive, G. G., Ujwal, M. L., Weitzman, C., Wu, J., & Zen, K. (1994) *J. Exp. Biol. 196*, 183−195.
Kunkel, T. A., Roberts, J. D., & Zakour, R. A. (1987) *Methods Enzymol. 154*, 367−382.
Lee, G. F., Dutton, D. P., & Hazelbauer, G. L. (1995) *Proc. Natl. Acad. Sci. U.S.A. 92*, 5416−5420.
Matsudaira, P. (1994) *Semin. Cell Biol. 5*, 165−174.
Matsudaira, P., Jakes, R., Cameron, L., & Atherton, E. (1985) *Proc. Natl. Acad. Sci. U.S.A. 82*, 6788−6792.
McKnight, C. J., Doering, D. S., Matsudaira, P. T., & Kim, P. S. (1996) *J. Mol. Biol. 260*, 126−134.
Milligan, D. C., & Koshland, D. E., Jr. (1988) *J. Biol. Chem. 263*, 6268−6275.
O'Shea, E. K., Rutkowski, R., Stafford, W. F., & Kim, P. S. (1989) *Science 245*, 646−648.
Otto, J. J. (1994) *Curr. Opin. Cell Biol. 6*, 105−109.
Pakula, A. A., & Simon, M. I. (1992) *Proc. Natl. Acad. Sci. U.S.A. 89*, 4144−4148.
Pope, B., Way, M., Matsudaira, P. T., & Weeds, A. (1994) *FEBS Lett. 338*, 58−62.
Rana, A., Ruff, P., Maalouf, G., Speicher, D., & Chishti, A. (1993) *Proc. Natl. Acad. Sci. U.S.A. 90*, 6651−6655.
Rosenberg, A. H., Lade, B. N., Chui, D., Lin, S., Dunn, J. J., & Studier, F. W. (1987) *Gene 56*, 125−135.
Simenel, C., Rose, T., Goethals, M., Vandekerckhove, J., Friederich, E., Louvard, D., & Delepierre, M. (1995) *Int. J. Pept. Protein Res. 45*, 574−586.
Studier, F. W., & Moffat, B. A. (1986) *J. Mol. Biol. 189*, 113−130.
Wells, J. A. (1991) *Methods Enzymol. 202*, 390.

BI9615699